Dalton Transactions

PAPER

View Article Online
View Journal | View Issue

Cite this: *Dalton Trans.*, 2015, **44**, 182

Structural, optical and sensing properties of novel Eu(III) complexes with furan- and pyridine-based ligands†

Fabio Piccinelli,*[a] Marco Bettinelli,[a] Andrea Melchior,*[b] Cristian Grazioli[b] and Marilena Tolazzi[b]

Received 31st July 2014,
Accepted 21st October 2014

DOI: 10.1039/c4dt02326a

www.rsc.org/dalton

A new family of imine and amine-based racemic ligands containing furan or pyridine as an aromatic donating ring [*N*,*N*′-bis(2-pyridylmethylidene)-1,2-(*R*,*R* + *S*,*S*)-cyclohexanediamine, **L1**; *N*,*N*′-bis(2-furanylmethylidene)-1,2-(*R*,*R* + *S*,*S*)-cyclohexanediamine, **L2**; *N*,*N*′-bis(2-pyridylmethyl)-1,2-(*R*,*R* + *S*,*S*)-cyclohexanediamine, **L3**; and *N*,*N*′-bis(2-furanylmethyl)-1,2-(*R*,*R* + *S*,*S*)-cyclohexanediamine, **L4**] and their trifluoromethanesulphonate ($CF_3SO_3^-$, OTf^-) and nitrate Eu(III) complexes is studied in acetonitrile (AN) solution. The stoichiometry and stabilities of the formed complexes are obtained by means of spectrophotometric titrations: when Eu(III) triflate is used as a starting salt, two mononuclear species (1 : 1 and 1 : 2) are detected, while only the 1 : 1 complex is observed when the nitrate salt is employed. The stability of these complexes, as well as the geometry of their Eu(III) environment, is significantly dependent on the nature of the ligand employed (imine or amine, furan or pyridine-based). DFT calculations show that all donor atoms are coordinated to the metal ion in the 1 : 1 Eu**L** (**L** = **L1–L4**) species and suggest that the higher stability of the complexes with **L1** and **L2** with respect to **L3** and **L4** is mostly due to the higher degree of preorganization of the former species. The optical response of the imine-based **L1** and **L2** Eu complexes, produced by NO_3^- coordination, has been studied in order to assess their application as sensing devices. With both ligands, an increase of the emission intensity on the addition of the nitrate ion is observed. This is higher for the Eu**L2** complex and underlines the important role of the nature of the heteroaromatic ring. Finally, it is worth noting that an efficient energy transfer process from the ligand to the metal is present in the case of the 1 : 1 triflate Eu(III) complex with the ligand **L1**.

Introduction

Lanthanide complexes have been extensively used in the last few decades as luminescent chemosensors for medical diagnostics and optical cell imaging,[1–3] contrast reagents for magnetic resonance imaging,[4–6] shift reagents for NMR spectroscopy,[7] as well as for applications in fundamental and applied science such as organic synthesis, bioorganic chemistry and catalysis.[8]

These applications have been made possible by the increased knowledge of fundamental properties (electronic, spectroscopic, thermodynamic, magnetic, and structural) of these ions, achieved as a consequence of the rapid development of fundamental studies on the lanthanide coordination chemistry. In this context, many solution studies have been carried out to obtain a detailed description of the speciation and formation thermodynamics of Ln(III) complexes in aqueous solutions[9,10] and organic solvents.[11–15]

As far as biomedical imaging applications are concerned, Eu(III) (and Tb(III)) complexes exhibit several desirable characteristics when compared with conventional organic fluorophores, such as long excited state lifetimes (usually in the milliseconds range), large energy shift between absorbed and emitted radiations (in the case of ligand sensitization) and very narrow emission bands; these two effects allow the separation of Ln(III) luminescence and the short-lived background fluorescence.[16] Eu(III) and Tb(III) complexes have also been extensively exploited as sensors of anions both in aqueous solution and in organic solvents. In this context, a possible approach to the anion recognition envisages the bonding of the anion at the metal center, displacing a coordinated solvent molecule or a weakly bound donor ligand. In the case of Eu(III) complexes the perturbation of the metal coordination environment can be evidenced by a change of the luminescence features of the metal ion.

[a]*Laboratorio Materiali Luminescenti, DB, Università di Verona, and INSTM, UdR Verona, Strada Le Grazie 15, 37134 Verona, Italy. E-mail: fabio.piccinelli@univr.it*
[b]*Dipartimento di Chimica, Fisica e Ambiente, Università di Udine, via Cotonificio 108, 33100 Udine, Italy. E-mail: andrea.melchior@uniud.it*

†Electronic supplementary information (ESI) available. See DOI: 10.1039/c4dt02326a

In a recent study,[17] we focused our attention on the racemic mixture of the pyridine-based chiral ligand *N*,*N*′-bis(2-pyridylmethylidene)-1,2-(*R*,*R* + *S*,*S*)-cyclohexanediamine (**L1**) and its novel trifluoromethanesulphonate ($CF_3SO_3^-$, OTf^-) and nitrate Eu(III) complexes. The nature of the species in acetonitrile (AN) solution was carefully analysed by means of spectrophotometric UV/Vis titration, Eu(III) luminescence and IR spectroscopy.

Among the aromatic donor groups, furan has attracted scarce attention in the field of coordination chemistry, probably due to its poor coordination ability (Donor Number, DN_{furan} = 6, $DN_{pyridine}$ = 33.1).[18] To the best of our knowledge, the coordination chemistry of furanyl-based ligands has been mostly studied with Co(II), Cu(II), Ni(II) and Zn(II) ions[19] with only two contributions presented for lanthanide ion complexes,[20,21] despite the importance of heterocyclics, such as furan, as conjugation bridges able to enhance luminescence properties. In those studies, the catalytic properties[20] and reactivity[21] of lanthanide complexes with furfuryl-functionalized indenyl ligands have been analysed, but a deep study of the coordination ability of the ligand was lacking, which was beyond the scope of that article.

In the present work, the previous study in an AN solution[17] has been extended to Eu(III) complexes with a new amino-pyridine ligand, *N*,*N*′-bis(2-pyridylmethyl)-1,2-(*R*,*R* + *S*,*S*)-cyclohexanediamine, **L3**, and the furanyl-based ones, *N*,*N*′-bis(2-furanylmethylidene)-1,2-(*R*,*R* + *S*,*S*)-cyclohexanediamine, **L2**, and *N*,*N*′-bis(2-furanylmethyl)-1,2-(*R*,*R* + *S*,*S*)-cyclohexanediamine, **L4** (Scheme 1). The effects of the substitution of a relatively strong donating ring (pyridine) with a poor donating one (furan) in the ligand backbone (Scheme 1) and of the different conformational flexibility of the ligands on the structure, stability and optical properties of the formed complexes have been investigated. A careful characterization of the nature and stability of the species in solution has been performed by spectrophotometry, luminescence and FT-IR spectroscopy. Density functional theory (DFT) calculations have been carried out to obtain information at a molecular level about the structure and coordination modes of these ligands with Eu(III). As far as the coordination chemistry of Ln(III) ions with ligands containing furan moieties is concerned, this work is the first study available with this unique combination of thermodynamic/luminescence/DFT methods.

Nitrate sensing by the imine-based **L1** and **L2** Eu complexes has also been studied by analyzing the evolution of the luminescence emission spectra upon the addition of tetraethylammonium nitrate to an AN solution of the Eu triflate complexes.

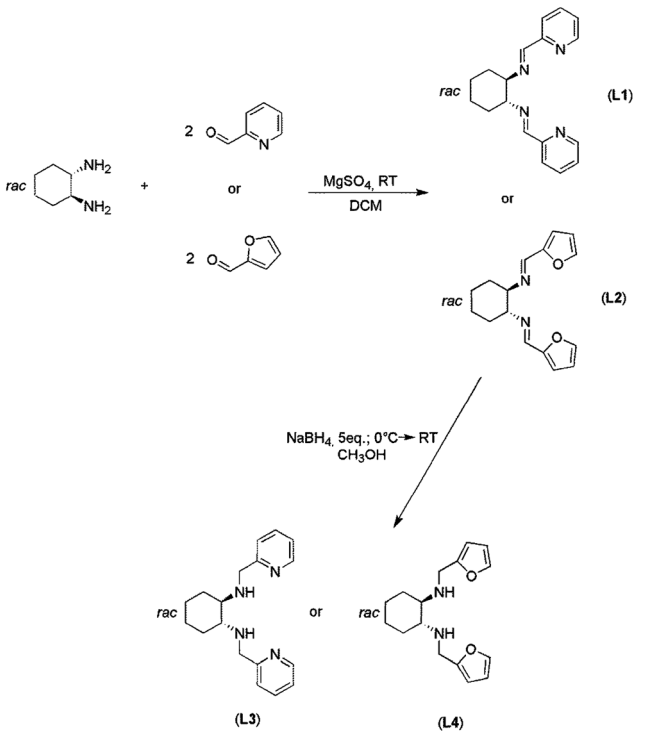

Scheme 1 Synthetic route employed to obtain **L1**–**L4** ligands.

Materials and methods

$Eu(OTf)_3$ (Aldrich, 98%) and $Eu(NO_3)_3{\cdot}5H_2O$ (Aldrich, 99.9%) have been stored under vacuum for several days at 80 °C and then transferred to a glove box. Stock solutions of the salts were prepared by dissolving weighed amounts of them in anhydrous AN and then standardized by complexometry with EDTA.[22] Absolute ethanol (Aldrich, 99.9%) was used without further manipulation and anhydrous acetonitrile (Aldrich, 99%) was obtained by refluxing for 2 hours in the presence of CaH_2. The central fraction was transferred to an MB 150 glove box and stored in the presence of molecular sieves (4 Å). The concentration of water (<5 ppm) was checked by the Karl Fischer method (Metrohm). Tetraethylammonium nitrate (Aldrich, 98%), used for sensing experiments, was used as such and stored in the glove box.

Synthesis and characterization

N,*N*′-bis(2-pyridylmethylidene)-1,2-(*R*,*R* + *S*,*S*)-cyclohexanediamine (**L1**) was obtained as previously reported.[17,23]

N,*N*′-bis(2-furanylmethylidene)-1,2-(*R*,*R* + *S*,*S*)-cyclohexanediamine (**L2**) (racemic mixture) was obtained by adding, in dichloromethane as a solvent, (±)-*trans*-1,2-cyclohexanediamine (1 eq.) and 2-furaldehyde (2 eq.) in the presence of anhydrous $MgSO_4$ as a dehydrating agent. The reaction mixture was stirred overnight, the $MgSO_4$ was filtered off and a pale yellow solid was obtained after the removal of the solvent under reduced pressure. The desired pure product was obtained after crystallization from the hexane solution of the crude product.

N,*N*′-bis(2-pyridylmethyl)-1,2-(*R*,*R* + *S*,*S*)-cyclohexanediamine (**L3**) and *N*,*N*′-bis(2-furanylmethyl)-1,2-(*R*,*R* + *S*,*S*)-cyclohexanediamine (**L4**) were obtained by following the synthetic protocol reported in the literature.[23] In Scheme 1 the synthetic procedures are summarized.

L2: Yield 82%. Elemental Anal. Calc. for $C_{16}H_{18}N_2O_2$ (MW 270.33): C, 71.09; H, 6.71; N, 10.36; O, 11.84. Found: C, 71.00;

H, 6.38; N, 10.33; O, 11.78. The nature of the ligand was confirmed using powder X-ray diffraction. The pattern is compatible with the following crystal data belonging to the same ligand synthesized by means of a different synthetic protocol:[24] monoclinic, space group $P2_1/n$, a = 9.4647(2), b = 9.9534(2), c = 15.7079(4) Å, β = 98.5090(10)°, V = 1463.49(6) Å^3.

L3: Characteristic data as reported in ref. 23.

L4: Yield 87%. Elemental Anal. Calc. for $C_{16}H_{22}N_2O_2$ (MW 274.36): C, 70.04; H, 8.08; N, 10.21; O, 11.66. Found: C, 70.00; H, 8.02; N, 10.25; O, 11.61. ^{1}H-NMR (Gemini spectrometer at 300 MHz using $CDCl_3$ as a solvent): δ 7.36 (s, 2H), 6.33 (d, J 4 Hz, 2H), 6.19 (d, J 4 Hz, 2H), 3.88 (d, J 16 Hz, 2H), 3.73 (d, J 16 Hz, 2H), 2.25 (m, 2H), 2.06 (m, 2H), 1.73 (m, 2H), 1.24 (m, 2H), 1.05 (m, 2H). ^{13}C-NMR (Gemini spectrometer at 300 MHz using $CDCl_3$ as a solvent): δ 25.13, 31.57, 43.72, 60.83, 106.52, 110.26, 141.66, 154.82. ESI-MS (Scan ES+; m/z): 298 ($[L + Na]^+$), 275($[L + H]^+$).

Complex Eu**L2**$(NO_3)_3$: (0.02 mmol dm^{-3} in anhydrous AN, direct mixture of **L2** and Eu$(NO_3)_3$). ESI-MS (Scan ES+; m/z): 631 ($[M + Na]^+$), 546 ($[M - NO_3]^+$).

Complex Eu**L3**$(NO_3)_3$: (0.02 mmol dm^{-3} in anhydrous AN, direct mixture of **L3** and Eu$(NO_3)_3$). ESI-MS (Scan ES+; m/z): 657 ($[M + Na]^+$), 572 ($[M - NO_3]^+$).

Complex Eu**L4**$(NO_3)_3$: (0.02 mmol dm^{-3} in anhydrous AN, direct mixture of **L4** and Eu$(NO_3)_3$). ESI-MS (Scan ES+; m/z): 661 ($[M + Na]^+$), 576 ($[M - NO_3]^+$).

Elemental analysis was carried out using an EACE 1110 CHNO analyzer. The ESI-MS spectra were obtained using a single-quadrupole mass spectrometer: for triflate complexes in AN solution they are not informative because a complex pattern of signals was detected and therefore no clear information about the molecular weight of the species in solution is provided.

FT-IR measurements

FT-IR spectra were recorded under nitrogen purge at 25 °C on a Bruker Vector 22 spectrometer. For these measurements a single cell with barium fluoride windows and 28 μm optical path length (determined by the interference fringes method) has been used. The cell was filled in the glove-box, tightly closed, and transferred into the spectrometer cavity with a sealed container. The solvent background was subtracted from the solution spectra which have been converted to absorbance units.

Spectrophotometric titrations

UV-Vis titrations were performed by adding a solution of Eu(III) salt to a ligand solution prepared with anhydrous AN. Typically, the concentration of the ligand was in the range of 2–5 × 10^{-5} mol dm^{-3}. To have a good number of points in a large $R_c = C_L/C_{Eu(III)}$ interval, at least two titrations per Eu^{3+}/**L2–4** system were carried out either with the metal or the ligand in the cell. The stability constant values were calculated by simultaneous fitting of the absorbance values at different wavelengths for two titrations, using the programs HypSpec[25] and Solverstat/EST tools[26,27] for the statistical analysis of the results.

For the ligands **L2**, **L3**, and **L4**, the molar extinction coefficients (ε) at the maximal wavelengths (λ/nm) are: for **L2**, ε_{258} = 3.51 × 10^4 mol L^{-1} cm^{-1}; for **L3**, ε_{199} = 4.5 × 10^4 mol L^{-1} cm^{-1} and ε_{258} = 9.1 × 10^3 mol L^{-1} cm^{-1}; for **L4**, ε_{212} = 2.04 × 10^4 mol L^{-1} cm^{-1}.

Luminescence

Room temperature emission and excitation spectra and the emission decay curves were measured using a Fluorolog 3 (Horiba-Jobin Yvon) spectrofluorimeter equipped with a Xe lamp, a double excitation monochromator, a single emission monochromator (mod. HR320) and a photomultiplier in photon counting mode for the detection of the emitted signal. The emission spectra were recorded upon "direct" excitation of Eu(III) ($^5D_0 \rightarrow {}^5L_6$; 395 nm).

DFT calculations

Geometry optimizations of the ligands and [Eu(**L1–4**)-$(CH_3CN)_4]^{3+}$ complexes were carried out at the DFT level using the PBE[28,29] exchange–correlation functional as previously demonstrated to give good structural and thermochemical results for metal–ligand interactions, also involving f-block elements.[30,31] Geometry optimizations were carried out under vacuum using a 6-31G(d) basis set for the ligands while europium has been described using the quasi-relativistic small core Stuttgart-Dresden pseudopotential[32] and the relative basis set. Ligands and complexes were optimized maintaining a C_2 symmetry. The starting geometries of the ligands have been optimized considering both their *cis* and *trans* forms with respect to the X–C–C–N dihedral angle (X = N, O in the heteroaromatic ring) as starting points.

The calculation of the vibrational spectrum of the $CF_3SO_3^-$ anion (C_{3v} symmetry) in acetonitrile has been carried out using the PBE functional and the 6-31+G(d,p) basis set. In order to evaluate in a simple way the modification of the triflate vibrational spectrum after the coordination to a lanthanide cation, also the structure of the La(OTf)$^{2+}$ (C_s) adduct has been considered. Solvent effects have been included by means of the PCM model.[33] All calculations were carried out using the Gaussian09 program.[34]

Results and discussion

Speciation

The speciation and stability of the complexes formed with the ligands **L1–L4** have been determined by spectrophotometric UV-Vis titrations. The absorbance changes during the titration of AN solution of the furan-based ligand **L2** with Eu$(NO_3)_3$ and Eu$(OTf)_3$ are shown in Fig. 1. In Fig. S1 (in ESI†), the spectra of the amino-pyridine ligand **L3** and of the furan-based ligand **L4** with the two Eu(III) salts are also reported. The values of the formation constants determined for **L2–L4** are reported in Table 1, together with those previously obtained for **L1**.[17]

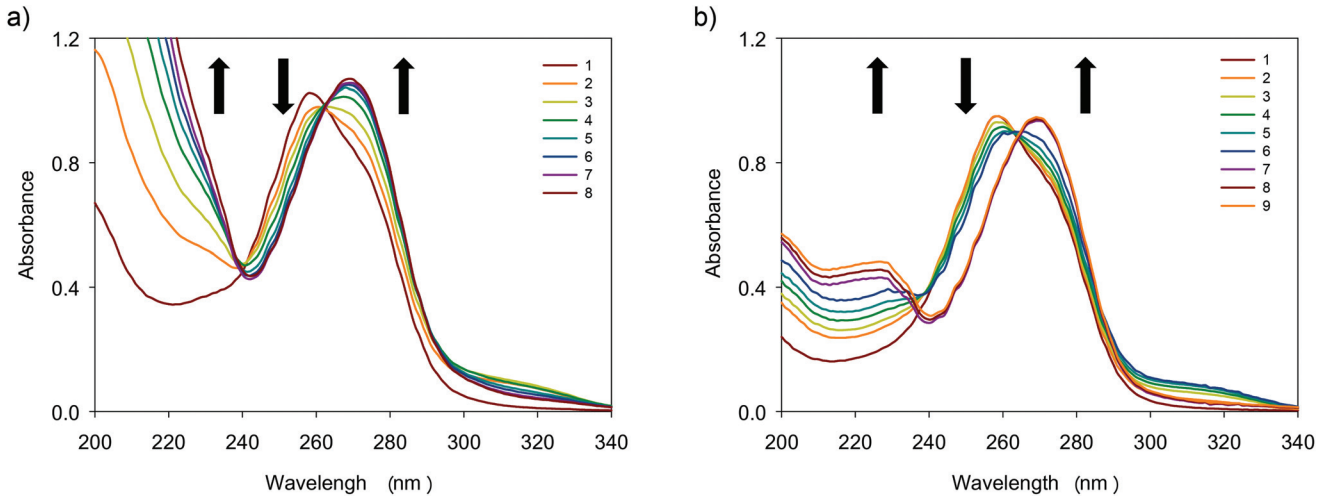

Fig. 1 Electronic spectra when **L2** (C_{L2} = 0.0292 mmol dm^{-3}, spectrum 1) is titrated with (a) $Eu(NO_3)_3$ (C_{Eu} = 20.4 mmol dm^{-3}, 7 additions of 2 μL aliquots) final C_{Eu}/C_L = 2.4 (spectrum 8); (b) $Eu(OTf)_3$ (C_{Eu} = 11.4 mmol dm^{-3}, 8 additions of 2 μL aliquots) final C_{Eu}/C_L = 1.6 (spectrum 9).

Table 1 Overall stability constants ($\log \beta_j$, j = 1, 2) for the reaction Eu + jL ⇄ EuL_j (charges omitted, L = **L1–L4**) of the triflate and nitrate complexes in AN (3σ in parentheses)

Salt		**L1**[17]	**L2**	**L3**	**L4**
$Eu(NO_3)_3$	$\log \beta_1$	6.86 (0.07)	4.8 (0.2)	6.3 (0.3)	5.0 (0.2)
$Eu(OTf)_3$	$\log \beta_1$	9.03 (0.09)	8.5 (0.5)	7.5 (0.5)	5.45 (0.03)
	$\log \beta_2$	16.52 (0.06)	13.5 (0.5)	14.5 (0.5)	10.04 (0.06)

The speciation models yielding the best fit of the experimental absorbances show that all the ligands **L2–L4** form only one 1 : 1 species when the $Eu(NO_3)_3$ is used, while two species (1 : 1 and 1 : 2) are formed when the triflate salt is concerned (Table 1), as previously found for **L1**.[17] This is evident in Fig. 1a where an isosbestic point is present when **L2** is titrated with a solution of $Eu(NO_3)_2$: this is not the case when $Eu(OTf)_3$ is used (Fig. 1b). In the case of **L3** and **L4**, complex formation results in an increase of absorbance (Fig. S1†).

As previously discussed,[11] the nitrate anion shows high affinity for the lanthanide ions as compared to coordinating solvents (NO_3^- > DMSO (dimethylsulfoxide) > DMF (*N*,*N*-dimethylformamide) > H_2O > AN), resulting in a non-electrolyte behaviour of $Eu(NO_3)_3$ in anhydrous AN solutions.[35] Lanthanide triflate salts have been shown to be completely dissociated only at concentrations lower than 0.05 mmol dm^{-3} in anhydrous AN,[36] while at high salt concentrations (~30 mmol dm^{-3}) the prevalent species in AN are the undissociated salt and the 1 : 1 electrolyte $Ln(OTf)_2^+$.[37] At this concentration, the release of triflate ions does not occur in AN, even in the presence of a strong N-donor such as *n*-butylamine (DN = 42),[18] which binds the lanthanide ions only through a preferential loss of coordinated solvent molecules.[14] The $\log \beta_1$ values found with **L1–L4** are always significantly lower for the nitrate complex with respect to the triflate one, indicating that the coordination of the first ligand is disfavored by the presence of nitrate ions. The different stability and nature of the species formed with the two Eu(III) salts can be explained by the fact that the ligands have to compete with the strongly coordinating nitrate which inhibits the coordination of the second ligand molecule. In addition, when nitrate is present in the first coordination sphere of Eu(III), the positive charge of the cation is lowered, giving rise to weaker ion–dipole bonding interaction between Eu(III) and the ligand. This is not the case if the Eu(III) triflate salt is used, which is completely dissociated at the concentrations used here in the UV-Vis titrations.[36]

Data in Table 1 show that the pyridine-based complexes are more stable than furan-based ones: from a structural point of view, it is reasonable that all donor groups of the ligands are coordinated to the Eu^{3+} cation, as suggested by the relatively quite high values of all the stability constants. The differences in stability are likely closely related to the σ-donor ability of the aromatic donor rings (DN = 33.1 and 6 for pyridine and furan, respectively).[18]

To gain information on the Eu**L1–L4** structures, DFT calculations have been run on 1 : 1 species. No experimental solution studies on CN (coordination number) of lanthanides in AN are available, but quantum mechanical calculations[38] on $Ln(AN)_n^{3+}$ clusters (n = 1–15, Ln = La, Eu, Yb) support the preference for 8-fold coordination for Yb(III) while for the solid state structures of the solvates the CN goes from 9 for the heavier lanthanides to 8 for the lighter ones. However, in the solid state, Eu(III) forms dimeric species with CN = 8 with **L1**.[17] On this basis, the $[Eu\mathbf{L1–4}(AN)_4]^{3+}$ solvated species (CN = 8) have been optimized and their structures are reported in Fig. 2 together with those of the ligands **L1–L4**. The ligands bind the Eu^{3+} cation maintaining a quasi-planar arrangement and all donor atoms are coordinated to the lanthanide cation with bond distances (Table 2) in good agreement with those found for lanthanide complexes in the solid state with pyridines[17] and open chain ligands with the furyl moiety.[21]

Imine complexes are generally more stable than the corresponding amino ones. This trend is unexpected, as secondary

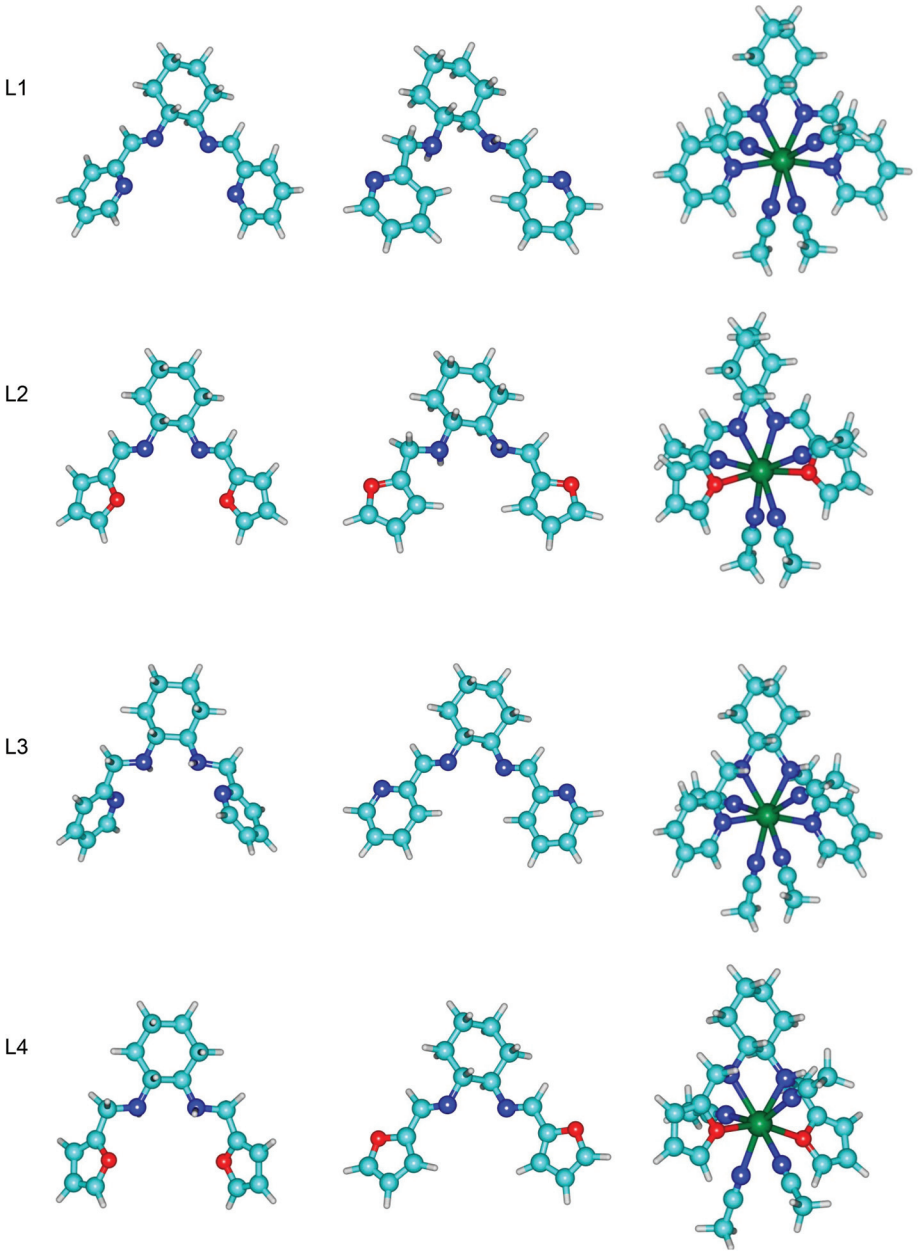

Fig. 2 Optimized geometries of **L1–L4** ligands (*cis* and *trans* isomers, left and middle columns) and Eu**L1–4** complexes (green = Eu, blue = N, light blue = C, red = O).

Table 2 Selected bond distances (Å) in the optimized structures of the Eu(III) complexes in Fig. 2

	L1	**L2**	**L3**	**L4**
Eu–N(imine)	2.495	2.450	—	—
Eu–N(amine)	—	—	2.540	2.524
Eu–N(pyridine)	2.532	—	2.515	—
Eu–O(furan)	—	2.565	—	2.483
Eu–N(CH_3CN)	2.550	2.522	2.561	2.534

amines are better σ-donors with respect to imines[39] and can be indicative of different counterbalancing effects influencing the final $\log \beta$ values. One factor on the basis of this result may be the lower solvation of the iminic ligands with respect to aminic ones (secondary amines form hydrogen bonds with the solvent molecules).[39] Furthermore, the higher preorganization of the more rigid imines may allow that the best conformation suitable for binding the Eu(III) cation should be reached with a lower energy cost and loss of conformational entropy. The optimization of the starting *cis* and *trans* forms (carried out including the PCM solvent) produced two sets of minimum structures (Fig. 2) showing no imaginary vibrational frequencies. The difference in energy between each pair of minimum structures (Fig. 2, Table S1†) indicates that, whereas for the furan-based ligands (**L2** and **L4**) there is no significant difference ($\Delta E_{\mathrm{isom}} = E_{cis} - E_{trans}$ = 0.2 and −0.3 kcal mol^{-1}), for the

pyridine-based (**L1** and **L3**) ligands the *trans* form is more stable (ΔE_{isom} = −5.4 and −1.6 kcal mol^{-1}, respectively). The reorganization energy of the ligand, that is, the difference between the energy of the ligand at the coordinates of the 1 : 1 complexes and its optimized geometry ($E_{reorg} = E_{ligand,complex} - E_{ligand,opt}$), has then been calculated (Table S1†). The E_{reorg} values for **L3** are higher with respect to **L1** when starting from the *cis* isomer (E_{reorg} = +2.9 and +7.6 kcal mol^{-1} for **L1** and **L3** respectively) and the same is found to occur for **L2** and **L4** (E_{reorg} = +3.8 and +6.0 kcal mol^{-1}, respectively). In the case of the *trans* isomer a similar result is obtained, with a slightly lower difference in E_{reorg} for the pyridines (E_{reorg} = +8.3 and +9.3 kcal mol^{-1} for **L1** and **L3**) and almost the same difference for **L2** and **L4** (E_{reorg} = +3.6 and +6.3 kcal mol^{-1}, respectively). This result clearly shows that the reorganization of the amine requires a higher energy cost with respect to the corresponding imine independently of the starting minimum structure (*cis* or *trans*). Furthermore, from an entropic point of view the more flexible amine ligands have a larger loss of conformational degrees of freedom. These two factors therefore give a good explanation for the higher log β values obtained for the triflate imine complexes with respect to the corresponding amines.

The analysis of spectra reported in Fig. 3 is useful for interpreting the coordination process of the ligands in the second coordination step in the high (and low) concentration range. In Fig. 3 the region of the vibrational spectrum relative to the triflate absorption is shown for a solution of Na(OTf) (a strong electrolyte in AN; red spectra in Fig. 3(a) and (b)) and for the **L2** and **L4** complexes with Eu(OTf)$_3$ in the concentration range of ~30 mmol dm^{-3}, where the salt is not completely dissociated.

In the Na(OTf) spectra, the bands at 1270, 1220 and 1155 cm^{-1} can be assigned to the stretching modes of ionic triflate in solution. On the basis of DFT calculations for the triflate ion (Fig. S2(a)†), the experimental band at 1270 cm^{-1} (Fig. 3, red) is assigned to the asymmetric stretching of SO_3 (calc. 1231 cm^{-1}) while that at 1155 cm^{-1} can be assigned to the symmetric stretching mode (calc. 1008 cm^{-1}). The theoretical spectrum presents an additional band at 1176 cm^{-1} and a shoulder at 1127 cm^{-1} associated with CF_3 and CS stretching modes. Therefore, modifications in the bands related to SO_3 stretching should be diagnostic of triflate coordination. In the spectrum of a Eu(OTf)$_3$ solution (reported only in Fig. 3(a), black) new bands appear at 1180, 1237 and 1323 cm^{-1}, which can be assigned to the coordinated triflate.[37] In particular, the band at 1323 cm^{-1} (Fig. 3(a), black) can be assigned to the SO_3 asymmetric stretching of the coordinated triflate, as confirmed by the calculated spectrum of the La(OTf)$^{2+}$ complex (Fig. S2(b)†) where the SO_3 stretching frequency is shifted from 1231 cm^{-1} to 1310 cm^{-1}. Also the experimental band at 1155 cm^{-1} (Fig. 3(a), black) can be assigned to the SO_3 symmetric stretching mode of the coordinated triflate (Fig. S2(b)†). By comparing the spectra (green lines in Fig. 3(a) and (b)) of solutions where only 1 : 1 complexes (and a small percentage of free Eu^{3+}) are present with those of Eu(OTf)$_3$ (black spectrum in Fig. 3(a)), it results that triflate is still coordinated to the cation. In contrast, when only Eu(**L2**)$_2$ and Eu(**L4**)$_2$ complexes

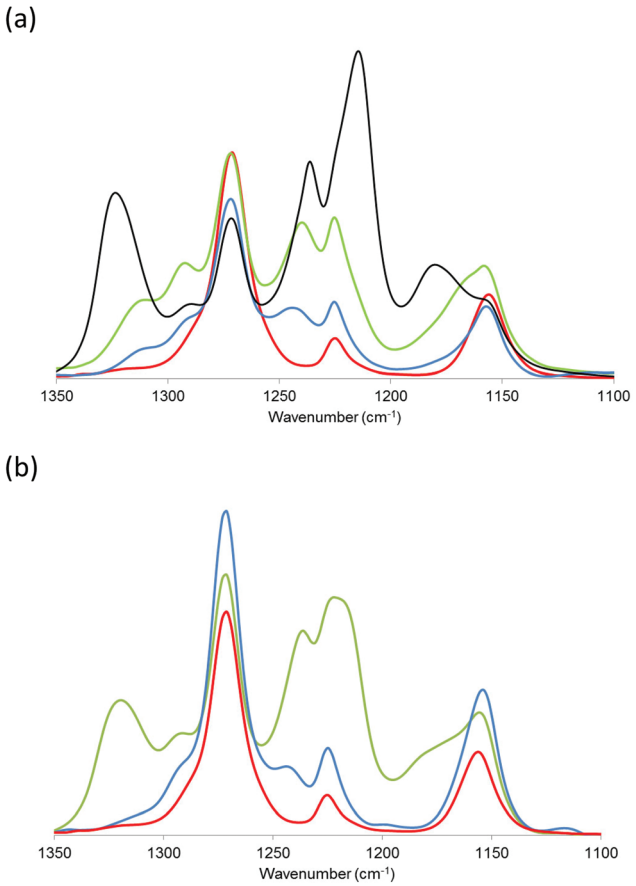

Fig. 3 IR spectra in the 1100–1350 cm^{-1} region of the solutions (all concentrations in mmol dm^{-3}): Na(OTf) 30.1 (red) in (a) and (b); (a) Eu(OTf)$_3$ C_{Eu} = 28.1 (black); Eu(OTf)$_3$/**L2** C_{Eu} = 34.8, C_{L2} = 25.3 (green); Eu(OTf)$_3$/**L2** C_{Eu} = 20.1, C_{L2} = 40.5 (blue); (b) Eu(OTf)$_3$/**L4** C_{Eu} = 33.8, C_{L4} = 27.1 (green); (b) Eu(OTf)$_3$/**L4** C_{Eu} = 19.80, C_{L4} = 42.1 (blue).

are present (Fig. 3(a) and (b), blue lines) the band pattern of the free ionic triflate is recovered. It is thus shown that the ligands studied are able to completely displace the triflate anion from the inner coordination sphere of the Eu(III) cation when 1 : 2 species are formed even at high triflate concentrations. Therefore, it can be reasonably proposed that the ligands are completely coordinated to the lanthanide at the low concentrations used in the spectrophotometric titrations, where the triflate anions are dissociated. This result can be extended also to **L1** and **L3** 1 : 2 complex formation, ligands where furan is substituted by the more coordinating pyridine.

Luminescence spectroscopy in AN solution

Triflate and nitrate complexes have also been investigated through luminescence spectroscopy. In the case of nitrate complexes, an anhydrous AN solution was prepared with the same content of Eu(III) and the ligand (1 mmol dm^{-3}) since the main species present in solution is the 1 : 1 Eu**L**(NO$_3$)$_3$ compound.

As far as the triflate complexes are concerned, anhydrous AN solutions were prepared with the same Eu(III) content (1 mmol dm^{-3}) and different stoichiometric ratios of the

ligand: in particular, for **L2**: two solutions with 1 : 1 and 2 : 1 ligand to metal mole ratios; for **L3**: two solutions with 0.5 : 1 and 2 : 1 ligand to metal mole ratios; and finally, for **L4**: two solutions with 0.5 : 1 and 3 : 1 ligand to metal mole ratios. At 1 mmol dm^{-3}, the equilibrium constants (Table 1) indicate the species distribution reported in Table S2.†

Nitrate complexes

The inner coordination sphere of the nitrate complexes (imine and amine-based) with pyridine-based ligands, **L1** and **L3**, was found to be constituted in the solid state of one ligand molecule, chelating the metal by four nitrogen atoms and three nitrate anions.[23] This coordination sphere is maintained also in AN solution in a wide range of concentrations (0.01–2.0 mmol dm^{-3}) for the imine derivative.[17] The luminescence emission spectra in AN solution of these Eu**L**$(NO_3)_3$ complexes (**L** = **L1** and **L3**) are shown in Fig. 4. They are very similar and the dominant $^5D_0 \rightarrow {}^7F_2$ emission band for both complexes is indicative of a strongly distorted Eu(III) environment. In fact, the asymmetry ratio, R:[40,41]

$$R = \frac{I(^5D_0 \rightarrow {}^7F_2)}{I(^5D_0 \rightarrow {}^7F_1)}$$

indicative of the degree of asymmetry of the coordination polyhedron around the Eu(III) ion, is very similar, namely, 6.26 and 5.95 for Eu**L1**$(NO_3)_3$ and Eu**L3**$(NO_3)_3$, respectively. The quite similar effective local symmetry at the Eu(III) ion indicates the close resemblance between the coordination geometry of pyridine-based ligands, regardless of the presence of an imine or amine group. The IR data of Eu**L3**$(NO_3)_3$ in AN solution clearly showed the exclusive presence of the undissociated nitrate ligand bound to Eu(III) in a bidentate coordination mode (absorption at 818 cm^{-1}),[42] as in the case of the imine derivative.[17] In conclusion, one ligand molecule and three nitrate anions should be assembled around the Eu^{3+} ion also for the Eu**L3**$(NO_3)_3$. Finally, the lifetimes of the $^5D_0$ emitting level extracted from the experimental curves (data not reported) clearly show a large difference between the imine (τ_{obs} = 1.21 ms) and amine (0.27 ms) complexes, indicating that multiphonon relaxation due to high frequency vibrations[43] is not operative in the imine-based ligand, as expected from the absence of N–H groups. On the other hand, for Eu**L3**$(NO_3)_3$ containing an amine ligand, the presence of two N–H amino groups in close proximity to the metal ion induces efficient non-radiative relaxation resulting in such a short lifetime.

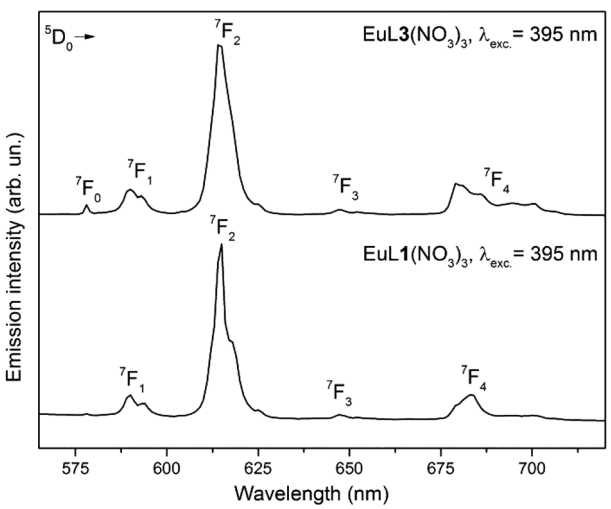

Fig. 4 Luminescence emission spectra of Eu**L**$(NO_3)_3$ (Eu(III) concentration of 1 mmol dm^{-3}) for pyridine-based complexes (Eu**L1**$(NO_3)_3$ and Eu**L3**$(NO_3)_3$).

The emission features do not change significantly if the furan-based ligands (**L2** and **L4**) are employed (Fig. S3, ESI†) even when the degree of distortion of the polyhedron around the Eu(III) ion increases. In particular, the R values are 6.64 and 6.98 for Eu**L2**$(NO_3)_3$ and Eu**L4**$(NO_3)_3$, respectively. The presence of two N–H amino groups in close proximity to the metal ion induces the presence of a non-radiative relaxation mechanism resulting in a shorter lifetime (τ_{obs} = 0.45 ms) for Eu**L4**$(NO_3)_3$ than for Eu**L2**$(NO_3)_3$ (τ_{obs} = 0.61 ms). In conclusion, the high degree of distortion of the Eu(III) geometric environments of all the nitrate complexes (Eu**L**$(NO_3)_3$; **L** = **L1**–**L4**) is assumed to be related to a crowded inner coordination sphere constituted by three bidentate nitrate anions and one tetradentate ligand molecule.

Triflate complexes

EuL species. As mentioned before, in order to study the luminescence spectroscopy of Eu**L**, solutions containing mainly the 1 : 1 species have been prepared, following the mole ratios reported in Table S1.† In the case of Eu**L3**$(OTf)_3$ and Eu**L4**$(OTf)_3$, a significant amount of free Eu(III) ions (not bound to the ligand molecule) is also present in solution. Therefore, its emission spectrum (Fig. S4†) must be taken into account as far as the luminescence features of Eu**L** are discussed.

Within the Eu**L** triflate family, the comparison between the luminescence emission spectra of the imine-based complexes (Eu**L1**$(OTf)_3$ and Eu**L2**$(OTf)_3$, Fig. 5) underlines several interesting features. In particular, the presence of a strong donating ring such as pyridine within the ligand backbone, instead of a poorly donating one such as furan, gives rise to a more distorted Eu^{3+} environment (R = 2.33 and 1.16 for Eu**L1**$(OTf)_3$ and Eu**L2**$(OTf)_3$, respectively). In addition, in the case of the furan-based Eu**L2**$(OTf)_3$ complex, the high intensity of the $^5D_0 \rightarrow {}^7F_0$ emission peaks is related to the axial symmetry of the Eu(III) coordination sphere, typical of the C_n and C_{nv} point groups, which have been shown to generate strong 0–0 transitions.[44,45] The degree of distortion of the Eu(III) environment observed in the case of an imine-based ligand containing a pyridine ring (**L1**) is retained if the imine function is converted to the amine one (**L3**, R = 2.38) and if both the aromatic ring and the imine function are modified (furan-based amine ligand, **L4**; R = 1.93). In addition, the presence of the amine function in the ligand backbone induces axial symmetry of the Eu(III) environment, as observed by the presence of the $^5D_0 \rightarrow {}^7F_0$ emission peak in the Eu(III) luminescence emission

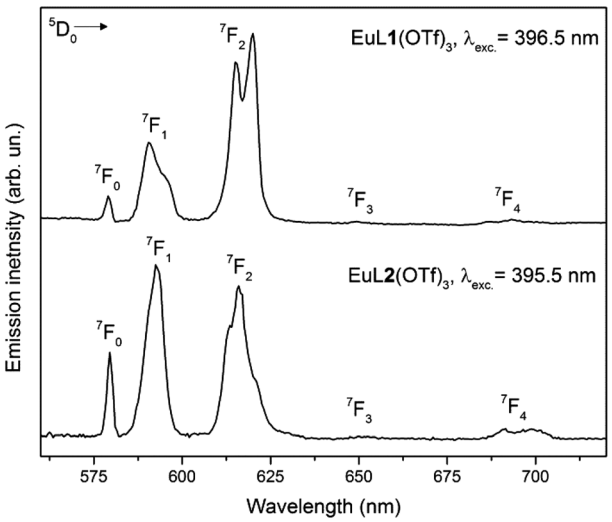

Fig. 5 Luminescence emission spectra of EuL triflates (Eu(III) concentration of 1 mmol dm^{-3}) for imine-based complexes containing the pyridine ring (Eu**L1**(OTf)$_3$) and the furan ring (Eu**L2**(OTf)$_3$).

spectra of Eu**L3**(OTf)$_3$ and Eu**L4**(OTf)$_3$ (Fig. S5, ESI†). In contrast with the emission spectra of the imine-based Eu**L1**(OTf)$_3$ and Eu**L2**(OTf)$_3$ complexes, a high intensity of the $^5D_0 \rightarrow {}^7F_4$ has been detected for amine-based Eu**L3**(OTf)$_3$ and Eu**L4**-(OTf)$_3$ complexes (Fig. S5, ESI†).

The lifetimes of the $^5D_0$ emitting level for the complexes containing the imine-based ligands (**L1** and **L2**) are compatible, as expected, with the presence in the inner coordination sphere of molecules able to induce an effective multiphonon relaxation process, such as acetonitrile (τ_{obs} = 0.45 ms for **L1** and τ_{obs} = 0.52 ms for **L2**). As far as the nature of the complexes in the case of amine-based ligands (**L3** and **L4**) is concerned, the values of the lifetimes of the $^5D_0$ emitting level are not informative, as a significant amount of free Eu(III) ions (not bound to the ligand molecule) is also present in solution (Table S2†).

Finally, for all Eu**L** species at 1 mmol dm^{-3} concentration, the presence of the triflate ion in the inner coordination sphere cannot be ruled out.

EuL_2 species. The concentration in solution of EuL_2 species has been maximized for each ligand employing the ligand to metal mole ratio reported in Table S2.† The luminescence emission features of these species are quite similar for the furan-based ligands **L2** and **L4**, and for the pyridine-based ligand containing the amine functional group (**L3**) (Fig. 6), underlining their similar Eu(III) geometric environments. In particular, they show a similar degree of distortion of the metal polyhedra (R = 2.16 for Eu**L2**$_2$(OTf)$_3$, R = 2.80 and 2.44 for Eu**L3**$_2$(OTf)$_3$ and Eu**L4**$_2$(OTf)$_3$, respectively) and significant $^5D_0 \rightarrow {}^7F_0$ and $^5D_0 \rightarrow {}^7F_4$ emission intensities. As mentioned above, the strong $^5D_0 \rightarrow {}^7F_0$ emission intensity is related to an axial symmetry of the Eu(III) coordination sphere. The presence of two N–H amino groups in close proximity to the metal ion, inducing a non-radiative relaxation mechanism in the case of Eu**L3**$_2$(OTf)$_3$ and Eu**L4**$_2$(OTf)$_3$, is confirmed by the short life-

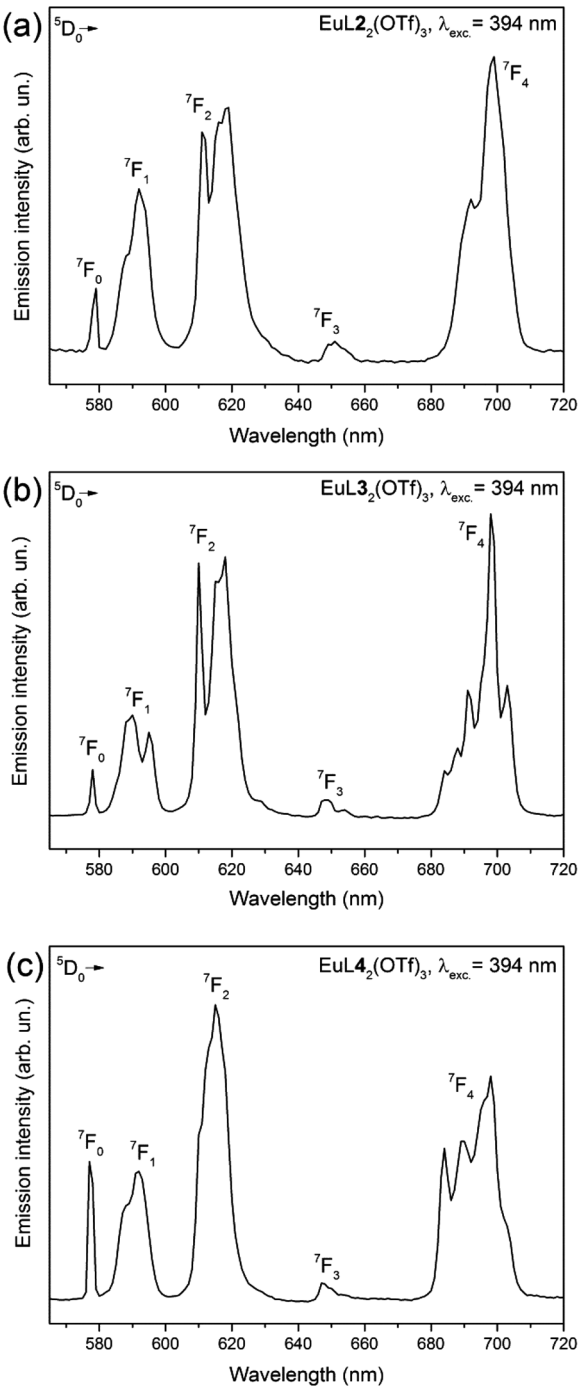

Fig. 6 Luminescence emission spectra of EuL_2 triflates (Eu(III) concentration of 1 mmol dm^{-3}) for: (a) the imine-based complex containing the furan ring (Eu**L2**$_2$(OTf)$_3$); (b) the amine-based complex containing the pyridine ring (Eu**L3**$_2$(OTf)$_3$); (c) the amine-based complex containing the furan ring (Eu**L4**$_2$(OTf)$_3$).

times of the $^5D_0$ emitting level extracted from the experimental curves (τ_{obs} = 0.19 ms and τ_{obs} = 0.18 ms, respectively).

In contrast, the higher values of the lifetimes (Eu**L1**$_2$(OTf)$_3$, τ_{obs} = 0.72 ms; Eu**L2**$_2$(OTf)$_3$, τ_{obs} = 0.65 ms) for the imine-based complexes confirm the presence of the two ligand molecules in the inner coordination sphere, hampering the coordi-

nation of molecules able to induce efficient multiphonon relaxation processes (acetonitrile or water molecules arising from the ambient moisture).

In conclusion, as far as the coordination geometry of the two ligand molecules in Eu**L**$_2$ species is concerned, it can be speculated that the highest flexibility of the amine-based ligands and/or the presence of a poorly coordinating aromatic ring (furan) in the ligand backbone gives rise to an axial symmetry at the metal and to a less distorted coordination environment when compared with that of the complex Eu**L1**$_2$(OTf)$_3$. In fact, in this case we obtained an asymmetry ratio of 4.35 and the 0–0 emission band cannot be detected.[17]

NO_3^- sensing experiments

It is well known that the radiationless deactivation process, occurring upon the interaction of OH, NH and, to a lesser extent, CH oscillators with the lanthanide ions, is extremely detrimental to the quantum efficiency of the rare earth ion luminescence (low ϕ values).[43] As far as sensing applications are concerned, where high values of the brightness ($\varepsilon\phi$) are required in order to detect traces of analytes, the imine-based ones (**L1** and **L2**) should be the best candidates among the ligands under investigation. In fact, due to the absence of OH, NH, or CH oscillators in close proximity to the luminescent metal ion of their Eu^{3+} complexes, the light emission efficiency, and consequently the quantum efficiency (ϕ), should be high.

In this context we have recorded the evolution of the luminescence emission spectra on the addition of a nitrate salt (tetraethylammonium nitrate) to an AN solution of the Eu**L1**(OTf)$_3$ and Eu**L2**(OTf)$_3$ triflate complexes. The direct excitation of Eu^{3+} cations was carried out to study the effect of the anion coordination on the lanthanide luminescence process. Due to the forbidden nature of this transition, the emission intensity is low and the concentration of Eu**L1**(OTf)$_3$ and Eu**L2**(OTf)$_3$ in solution cannot be lowered below 1 mmol dm^{-3}. Interestingly, in both cases an increase of the intensity of the emission peak around 616 nm on the addition of the nitrate anion has been observed (Fig. 7). The luminescence intensity of Eu**L2**(OTf)$_3$ was increased 7 times, whereas that relative to Eu**L1**(OTf)$_3$ only 1.8 times, by the addition of 4 equivalents of NO_3^-. This finding underlines the important effect of the nature of the heteroaromatic ring, and consequently of its donor ability, on the sensitivity of the nitrate detection.

Finally, an efficient intramolecular energy transfer from the triplet state of the coordinated organic ligand (*antenna effect*) to the excited state of Ln^{3+} ions is strongly required in order to provide a high ε value and bypass the parity-forbidden nature of the f–f transitions, characterized by a low ε value. In Fig. 8 the excitation spectra of the Eu**L** triflate complexes containing **L1** and **L2** ligands (Eu**L1**(OTf)$_3$ and Eu**L2**(OTf)$_3$, respectively) are shown. In the case of Eu**L1**(OTf)$_3$ the excitation band around 285 nm, due to a ligand to metal energy transfer process (antenna effect), effectively works, also for very low concentration of the complex (1 μmol dm^{-3}). The very strong intensity of this excitation band together with the potential

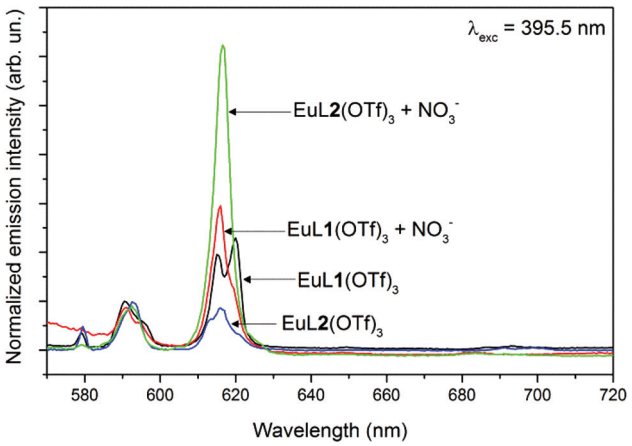

Fig. 7 Evolution of the luminescence emission spectra upon addition of the nitrate anion, for complexes Eu**L1**(OTf)$_3$ and Eu**L2**(OTf)$_3$. [Eu**L1**(OTf)$_3$] = [Eu**L2**(OTf)$_3$] = 1 mmol dm^{-3}; [NO_3^-] = 4 mmol dm^{-3}.

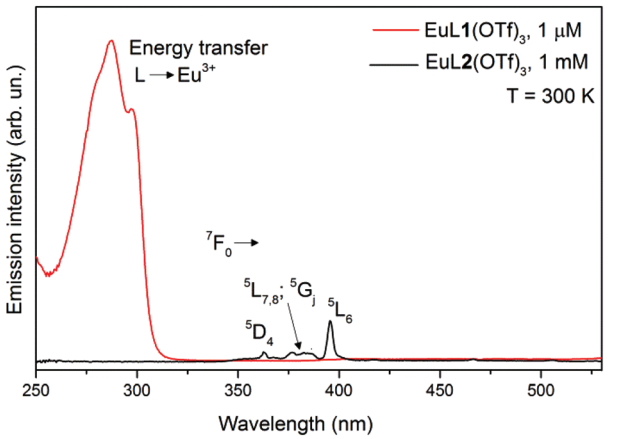

Fig. 8 Excitation spectra of Eu**L1**(OTf)$_3$ (λ_{em} = 614 nm) and Eu**L2**(OTf)$_3$ (λ_{em} = 615.5 nm). Slit width was adjusted to 2.5 nm for excitation and 5.0 nm for emission.

displacement, in the inner coordination sphere, of the weakly bound triflate ligand or solvent molecules by a donor species, suggests this compound as an efficient sensor of anions or molecules.

In contrast, the ligand **L2** is not able to induce an efficient antenna effect. For its complexes, the direct excitation of the Eu(III) ion (f–f transition around 395 nm) is the only efficient optical route to obtain light emission from the Eu(III) ion (Fig. 8). Unfortunately, although Eu**L2**(OTf)$_3$ shows a good sensitivity toward the nitrate anion, due to the forbidden nature of the f–f transition the emission intensity is low and the concentration of this species in solution cannot be lowered below 1 mmol dm^{-3}; as a consequence the limit of anion detection for this sensor is not particularly low.

Further work is in progress to extend the sensing experiments in several anions in AN and also in different organic solvents. In addition, exploiting the efficient antenna effect in the case of Eu**L1**(OTf)$_3$, experiments will be carried out in the micromolar range of anion concentration.

In the present contribution, we have focused our attention on the structural and optical properties of Eu(III) complexes, exploring all possible ligand to metal stoichiometric ratios. Nevertheless, with the aim of deeply investigating the sensing properties of a complex, the role of the anion stoichiometry must also be investigated. In fact, as reported in great detail by Montalti *et al.*,[46,47] from the variation in the absorption spectra of an acetonitrile solution of a triflate europium (or terbium) complex on the addition of anions, it is possible to calculate the cumulative association constants for the formation of complexes with one, two, or three anions (nitrate, chloride, fluoride and acetate). X-ray diffraction, as well as QM calculations, demonstrates the coordination of three nitrate anions in a bidentate mode and the step-by-step relegation of the bipy subunits of the investigated ligand in the second coordination sphere. Moreover, the authors have demonstrated the crucial effect of the anion stoichiometry on the efficiency of the energy-transfer processes from the ligand to the metal ion (Eu^{3+}), as well as on the optical emission features of the complex. For this reason, as far as the sensing properties of a lanthanide complex are concerned, it is worth pointing out that, apart from the obvious main role of the nature of the chromophoric ligand, there is a non-negligible effect of the anion stoichiometry.

Conclusion

In this paper a new family of pyridine-based and furan-based chiral racemic ligands and their triflate and nitrate Eu(III) complexes, of a simple synthetic approach, is presented. Both 1 : 1 and 1 : 2 compounds are formed by triflate salts, whereas only 1 : 1 species with $Eu(NO_3)_3$, due to the stronger coordination of the nitrate ion. The presence of the amine function in the ligand backbone, instead of the imine one, decreases the stability of the complexes, as well as the substitution of pyridine with furan. The analysis of the vibrational spectra of the europium triflate complexes with **L2** and **L4** in the high concentration range shows that the 1 : 1 complex still contains coordinated triflate(s) which is(are) completely displaced when the second ligand enters the coordination sphere of the metal ion. In agreement with DFT results, vibrational spectra support the fact that the ligands are completely coordinated to the Eu(III) ion also at the very low concentrations used in UV-Vis experiments, where triflate anions are dissociated.

The observed stability trend is due to several factors: the lower coordination ability of furan if compared with pyridine, the higher solvation of the amine ligands and their complexes with respect to iminic ones. Furthermore, the less preorganized amines pay a higher energy cost in order to reach the conformation suitable for binding the Eu(III) cation, as shown by DFT calculations.

From the inspection of the luminescence emission spectra of Eu(III) it clearly emerges that several factors affect the spectroscopic features of the luminescent ion: the nature of the heteroaromatic ring and the functional group (imine or amine). Among the investigated complexes the nitrate-based ones are characterized by the most distorted Eu(III) geometric environment, giving rise to a predominant $^5D_0 \rightarrow {}^7F_2$ luminescence emission band and high values of the asymmetry ratio ($R \sim 7$) for the aminic complex containing furan as the aromatic moiety.

The Eu(III) luminescence emission features are sensitive to the presence of the nitrate anion, in the case of both pyridine-based (Eu**L1**$(OTf)_3$) and furan-based (Eu**L2**$(OTf)_3$) triflate compounds. The sensitivity towards the nitrate anion is strongly dependent on the nature (donor ability) of the heteroaromatic ring within the ligand backbone. The poorer donating furan ring gives rise to a higher sensitivity.

Finally, it is worth underlining that a ligand to metal energy transfer process (*antenna effect*) is effectively present for Eu**L1**$(OTf)_3$, which can therefore be considered to be a good candidate for sensing applications.

Acknowledgements

The authors gratefully thank Erica Viviani and Serena Zanzoni for expert technical assistance and Veronica Paterlini for the Eu^{3+} spectroscopic measurements. CINECA is also gratefully acknowledged by A. M. for computing time, project "IscrC_HM2014".

References

1 J. C. G. Bünzli and C. Piguet, *Chem. Soc. Rev.*, 2005, **34**, 1048–1077.
2 I. Hemmila and V. Laitala, *J. Fluoresc.*, 2005, **15**, 529–542.
3 E. J. New, D. Parker, D. G. Smith and J. W. Walton, *Curr. Opin. Chem. Biol.*, 2010, **14**, 238–246.
4 P. Caravan, *Acc. Chem. Res.*, 2009, **42**, 851–862.
5 P. H. Fries, D. Imbert and A. Melchior, *J. Chem. Phys.*, 2010, **132**, 044502.
6 A. C. Mendonça, A. F. Martins, A. Melchior, S. M. Marques, S. Chaves, S. Villette, S. Petoud, P. L. Zanonato, M. Tolazzi, C. S. Bonnet, É. Tóth, P. Di Bernardo, C. F. G. C. Geraldes and M. A. Santos, *Dalton Trans.*, 2013, **42**, 6046–6057.
7 G. Otting, *J. Biomol. NMR*, 2008, **42**, 1–9.
8 M. Shibasaki and N. Yoshikawa, *Chem. Rev.*, 2002, **102**, 2187–2209.
9 C. Piguet and J. C. G. Bünzli, in *Handbook on the Physics and Chemistry of Rare Earths*, ed. A. G. Karl, Elsevier, 2010, vol. 40, pp. 301–553.
10 P. Di Bernardo, P. L. Zanonato, A. Bismondo, A. Melchior and M. Tolazzi, *Dalton Trans.*, 2009, 4236–4244.
11 P. Di Bernardo, A. Melchior, M. Tolazzi and P. L. Zanonato, *Coord. Chem. Rev.*, 2012, **256**, 328–351.
12 A. Cassol, G. R. Choppin, P. Di Bernardo, R. Portanova, M. Tolazzi, G. Tomat and P. L. Zanonato, *J. Chem. Soc., Dalton Trans.*, 1993, 1695–1698.

13 P. Di Bernardo, P. L. Zanonato, A. Melchior, R. Portanova, M. Tolazzi, G. R. Choppin and Z. Wang, *Inorg. Chem.*, 2008, **47**, 1155–1164.
14 A. Cassol, P. Di Bernardo, R. Portanova, M. Tolazzi and P. L. Zanonato, *Inorg. Chim. Acta*, 1997, **262**, 1–8.
15 N. Dalla-Favera, J. Hamacek, M. Borkovec, D. Jeannerat, F. Gumy, J. C. G. Bünzli, G. Ercolani and C. Piguet, *Chem. – Eur. J.*, 2008, **14**, 2994–3005.
16 J. C. G. Bünzli, *Chem. Rev.*, 2010, **110**, 2729–2755.
17 F. Piccinelli, A. Melchior, A. Speghini, M. Monari, M. Tolazzi and M. Bettinelli, *Polyhedron*, 2013, **57**, 30–38.
18 Y. Marcus, *The Properties of Solvents*, John Wiley and Sons, Chichester, 1998.
19 Z. H. Chohan, H. Pervez, A. Rauf, A. Scozzafava and C. T. Supuran, *J. Enzyme Inhib. Med. Chem.*, 2002, **17**, 117–122.
20 Y. Wu, S. Wang, C. Qian, E. Sheng, M. Xie, G. Yang, Q. Feng, L. Zhang and X. Tang, *J. Organomet. Chem.*, 2005, **690**, 4139–4149.
21 S. Arndt, T. P. Spaniol and J. Okuda, *Organometallics*, 2003, **22**, 775–781.
22 G. H. Jeffrey, J. Bassett, J. Mendham and R. C. Denney, *Vogel's textbook of quantitative chemical analysis*, John Wiley & Sons, 5th edn, 1990, vol. 14.
23 F. Piccinelli, A. Speghini, M. Monari and M. Bettinelli, *Inorg. Chim. Acta*, 2012, **385**, 65–72.
24 T. R. van den Ancker, G. W. V. Cave and C. L. Raston, *Green Chem.*, 2006, **8**, 50.
25 P. Gans, A. Sabatini and A. Vacca, *Talanta*, 1996, **43**, 1739–1753.
26 C. Comuzzi, P. Polese, A. Melchior, R. Portanova and M. Tolazzi, *Talanta*, 2003, **59**, 67–80.
27 S. del Piero, A. Melchior, P. Polese, R. Portanova and M. Tolazzi, *Ann. Chim.*, 2006, **96**, 29–49.
28 C. Adamo and V. Barone, *J. Chem. Phys.*, 1999, **110**, 6158–6170.
29 J. Perdew, K. Burke and M. Ernzerhof, *Phys. Rev. Lett.*, 1996, **77**, 3865–3868.
30 L. Cavallo, S. Del Piero, J.-M. Ducéré, R. Fedele, A. Melchior, G. Morini, F. Piemontesi, M. Tolazzi and J. M. Ducere, *J. Phys. Chem. C*, 2007, **111**, 4412–4419.
31 P. Di Bernardo, P. L. Zanonato, F. Benetollo, A. Melchior, M. Tolazzi and L. Rao, *Inorg. Chem.*, 2012, **51**, 9045–9055.
32 X. Cao and M. Dolg, *J. Chem. Phys.*, 2001, **115**, 7348.
33 J. Tomasi, B. Mennucci and R. Cammi, *Chem. Rev.*, 2005, **105**, 2999–3093.
34 M. J. Frisch, *et al.*, *Gaussian 09, Revis. A.02*, 2009.
35 J. C. G. Bünzli, J. P. Metabanzoulou, P. Froidevaux and L. P. Jin, *Inorg. Chem.*, 1990, **29**, 3875–3881.
36 A. F. D. de Namor, S. Chahine, O. Jafou and K. Baron, *J. Coord. Chem.*, 2003, **56**, 1245–1255.
37 P. Di Bernardo, G. R. Choppin, R. Portanova and P. L. Zanonato, *Inorg. Chim. Acta*, 1993, **207**, 85–91.
38 M. Baaden, F. Berny, C. Madic and G. Wipff, *J. Phys. Chem. A*, 2000, **104**, 7659–7671.
39 P. Di Bernardo, A. Melchior, R. Portanova, M. Tolazzi and P. L. L. Zanonato, *Coord. Chem. Rev.*, 2008, **252**, 1270–1285.
40 E. W. J. L. Oomen and A. M. A. van Dongen, *J. Non-Cryst. Solids*, 1989, **111**, 205–213.
41 R. Reisfeld, E. Zigansky and M. Gaft, *Mol. Phys.*, 2004, **102**, 1319–1330.
42 J. C. G. Bünzli, C. Mabillard and J. R. Yersin, *Inorg. Chem.*, 1982, **21**, 4214–4218.
43 *Radiationless Processes*, ed. B. DiBartolo and V. Goldberg, Plenum Press, New York, 1980.
44 R. Peacock, in *Rare Earths SE - 3*, Springer Berlin Heidelberg, 1975, vol. 22, pp. 83–122.
45 B. Piriou, D. Fahmi, J. Dexpert-Ghys, A. Taitai and J. L. Lacout, *J. Lumin.*, 1987, **39**, 97–103.
46 M. Montalti, L. Prodi, N. Zaccheroni, L. Charbonnière, L. Douce and R. Ziessel, *J. Am. Chem. Soc.*, 2001, **123**, 12694–12695.
47 L. J. Charbonnière, R. Ziessel, M. Montalti, L. Prodi, N. Zaccheroni, C. Boehme and G. Wipff, *J. Am. Chem. Soc.*, 2002, **124**, 7779–7788.